Electronic Supplementary Material (ESI) for Lab on a Chip.

Supplementary Materials

Deterministic droplet coding *via* acoustofluidics

Peiran Zhang,[a]# Wei Wang,[ab]# Hai Fu,[ac] Joseph Rich,[d] Xingyu Su,[a] Hunter Bachman,[a] Jianping Xia,[a] Jinxin Zhang,[a] Shuaiguo Zhao,[a] Jia Zhou,[b]*, and Tony Jun Huang[ad]*

[a] Department of Mechanical Engineering and Material Science, Duke University, Durham, NC 27708, USA. E-mail: tony.huang@duke.edu

[b] ASIC and System State Key Laboratory, School of Microelectronics, Fudan University, Shanghai 200433, P. R. China. E-mail: jia.zhou@fudan.edu.cn

[c] Department of Fluid Control and Automation, School of Mechanics Engineering, Harbin Institute of Technology, Harbin, Heilongjiang 150000, P. R. China

[d] Department of Biomedical Engineering, Duke University, Durham, NC 27708, USA.

# These authors contribute equally to this work.

* Correspondences should be addressed to Dr. Jia Zhou or Dr. Tony Huang.

Supplementary Note S1: Cutting of water stream with oil ejection actuated by TSAW pulse

Numerical simulations were developed to compare with experimental results of the acoustofluidic platform. To illustrate the splitting of aqueous flow by the oil jet under the effect of TSAW, a simplified 2D model has been developed using COMSOL Multiphysics® 5.2a. A two-phase laminar flow module was utilized for fluidic properties while two inlets were imposed with corresponding flow rates. To represent the pressure gradient induced by TSAW, a volume force domain condition was imposed on the oil chamber. The results of experimental measurements and numerical simulation are demonstrated in Fig. S1.

Supplementary Note S2: Coding protocols for droplet array

Based on the functionality we proposed, the width of the gap between two adjacent SAW pulses corresponds to the size of the dispensed water droplet. Thus, the length of droplets dispensed successively and their spatial arrangement by length is regulated by programming the length of the gap period in a sequence of SAW pulses. As shown in Fig. S2, the droplets are categorized into three collections as "0", "1", and "Gap" in increasing order of the droplet size, corresponding to an increasing gap period in their dispensing process. Herein, the length of the successively dispensed droplets is programmed following the arrangement of "110 – Gap – 101 – Gap – 101 – Gap – 0", which presents a binary word, "DUKE", in Morse Code. Moreover, a micrograph of another droplet array is presented in Fig. S3 where the size of successively dispensed droplets gradually decreases and cycles. The ability to precisely size dispensed droplets using acoustofluidics provides a powerful approach to automatically code a large number of droplet samples in complex environments.

Supplementary Note S3: Possible unique combinations of N droplets

As shown in Fig. 6, we have achieved robust encoding of droplets of four different volumes (*i.e.*, 0.75 nL, 1.5 nL, 3 nL, and 4.5 nL) using four different pulse durations (*i.e.*, 10 ms, 20 ms, 40 ms, and 60 ms), which corresponds to 4^N possible combinations for a droplet train consisting of N droplets in theory. Considering the possible overlapping of droplet volumes (Fig. 5a), binary codes (*i.e.*, 0.75 nL and 3 nL, or 1.5 nL and 4.5 nL) can be adopted to enhance robustness, theoretically leading to 2^N possible combinations for N droplets. The main limiting factor for generating a large set of unique combinations over a long time-scale is that the time-averaged volume of generated droplet needs to match with the pumping rate of the water syringe. Otherwise the accumulated pressure in the water channel over time will induce fluctuations of droplet volumes. Therefore, the theoretical combinations need to be at-most square-rooted using our current configuration in the worst-case

scenario (*i.e.*, $2^{N/2}$ or $4^{N/2}$), in which case the latter N/2 droplets can be used to compensate the volumes of former N/2 droplets to match water flowrate.

Supplementary Note S4: Discussion on error recovery

To robustly encode information into address bits in binary combinations of droplet lengths, the chosen pulse durations need to lead to sufficient separation in droplet volume to threshold the generated droplet bits for consistent readout. If the pulse-duration-associated droplet lengths are too close to each other (*e.g.*, 10 ms and 30 ms durations), coding or decoding errors may occur due to the rare events that a droplet is generated with the wrong volume. However, such rare events are conceived as general issues for droplet coding in microfluidics as well as electronic coding in telecommunications, where in the latter scenario the errors can be corrected by verification codes in the end of the bit packet. For enhancing the robustness of droplet coding, the following two redundant strategies can be adopted: (1) Adding droplet bits with precalculated combinations at the end of each droplet packet to verify the encoded information. (2) Encoding information into the address bits following specific rules. For example, we can encode the address bits following numeric order (*i.e.*, 1, 2, 3 …) but in binary codes, and thus we will discover the packet with the wrong address bit for correction or discarding.

Supplementary Note S5: Image-processing-based decoding strategy

To date, several sensing mechanisms including impedance sensing, optical sensing, capacitive sensing have been developed for the serial readout of droplets, which can be integrated to the downstream of the serpentine channel using photolithography during nanofabrication. Here we adopt image-processing to retrieve the information of droplet lengths from the video captured by a fast camera for device simplicity. The two curvatures of a flowing droplet can be detected and marked by the grey and black boxes. The length of the droplet therefore can be calculated by measuring the distances between the midpoints of the two boxes. The observation window can be shrunk to as small as the sizes of nanoliter droplets, which simultaneously increases the processing framerate to about 2,000 fps. Such imaging processing algorithm can also be applied in real-time videos to gate the trigger signals for sorting. However, the maximum framerate of real-time image processing will be reduced to 50 ~ 60 fps due to the inherent delays of instrument communications.

Supplementary Note S6: Potential applications based on acoustofluidic droplet coding unit

Since the serial processing functions of droplets (e.g., counting, imaging, injection, and sorting) have been well-established on microfluidic platforms, they can be easily integrated to the downstream of the droplet coding unit using photolithography. For example, a three-input (e.g., 2 drug inputs, 1 cell input) nozzle can be integrated upstream of the water channel to create 2D drug gradients in droplets with serial format. Each droplet packet (i.e., 50 droplets) will have unique address bits corresponding to different combinatorial drug concentrations which can be decoded easily by optical imaging. In this way, multiplexed conditions can be screened in a single run of experiment. Besides, the droplet coding platform is highly advantageous for the long-term monitoring of single cell kinetics beyond endpoint analysis since the cells can be consistently identified and tracked by locating the address bits (i.e., barcodes).

Supplementary Figures

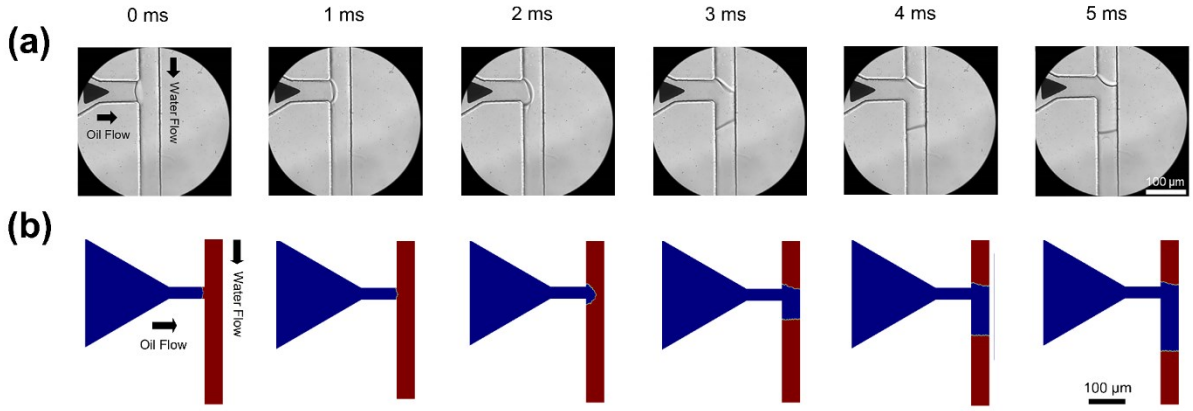

Figure S1. Cutting of water stream with oil ejection. (a) Micrographs of experiments. (b) Simulation results of the two-phase system. The oil flow was ejected from the chamber under the effect of surface acoustic waves, which cuts the water flow off to form a droplet in the downstream of the channel. The flow rates of water and oil are 4.5 $\mu L \cdot min^{-1}$ and 5 $\mu L \cdot min^{-1}$, respectively. The duration of TSAW pulse is 5 ms.

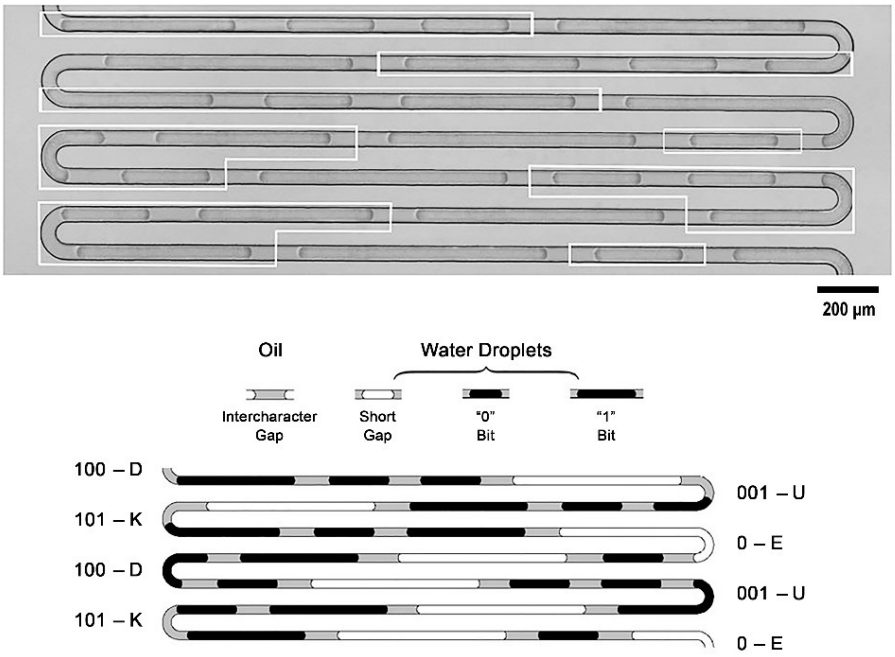

Figure S2. A droplet array dispensed by our acoustofluidic platform. Programmed acoustic pulses tuned the size and spatial arrangement of the droplet array. The micrograph and illustration for the droplet array are demonstrated here with the Morse code of "DUKE".

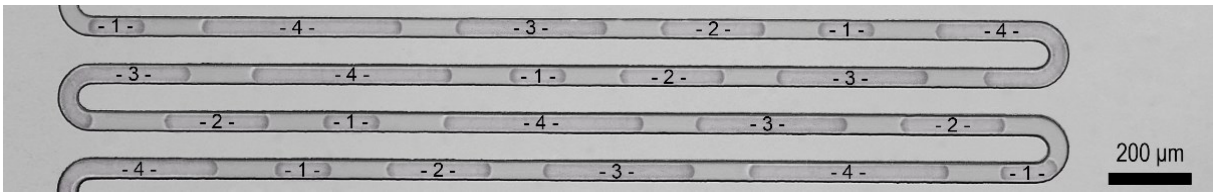

Figure S3. Micrograph of a droplet array dispensed by our acoustofluidic platform. The size of successively dispensed droplets decreases gradually and cycles.

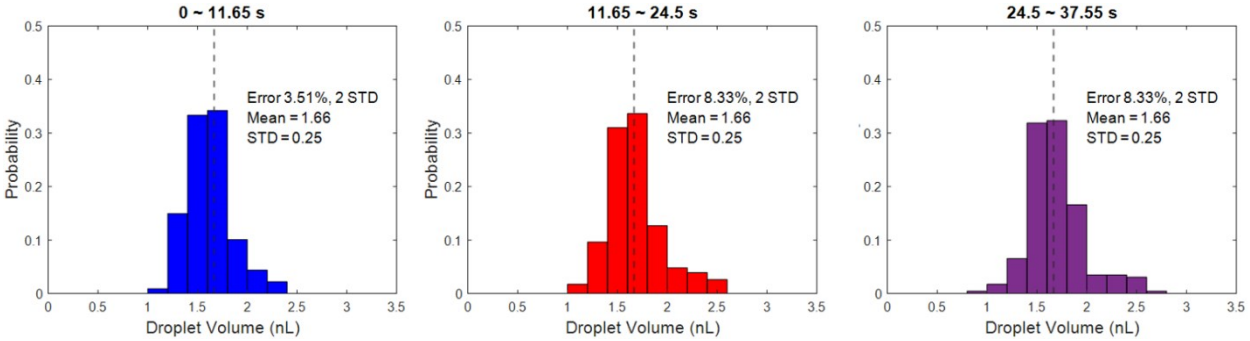

Figure S4. The time-lapsed distribution of droplet volume at a generation frequency of 20 Hz. The rate of generating droplets with abnormal volumes (*i.e.*, beyond 2 standard deviations) increase significantly after the first 11.65 seconds. The dashed line indicates the target droplet volume which matches with the flowrate of water (2 μL·min^{-1}).

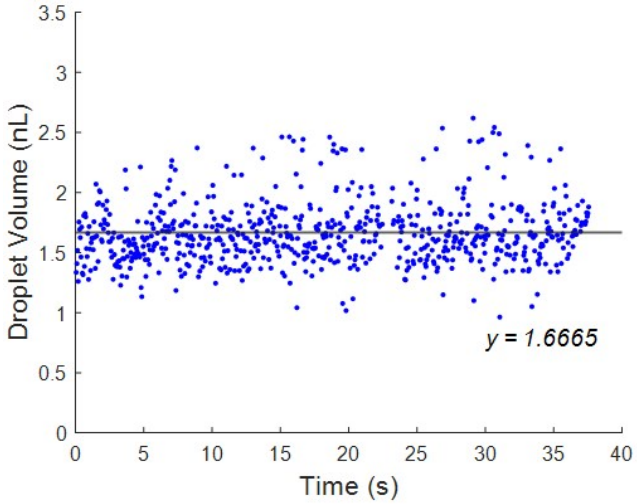

Figure S5. Volumes of droplets generated at different time points (20 Hz speed). The dashed line indicates the target droplet volume which matches with the flowrate of water (2 μL·min^{-1}).

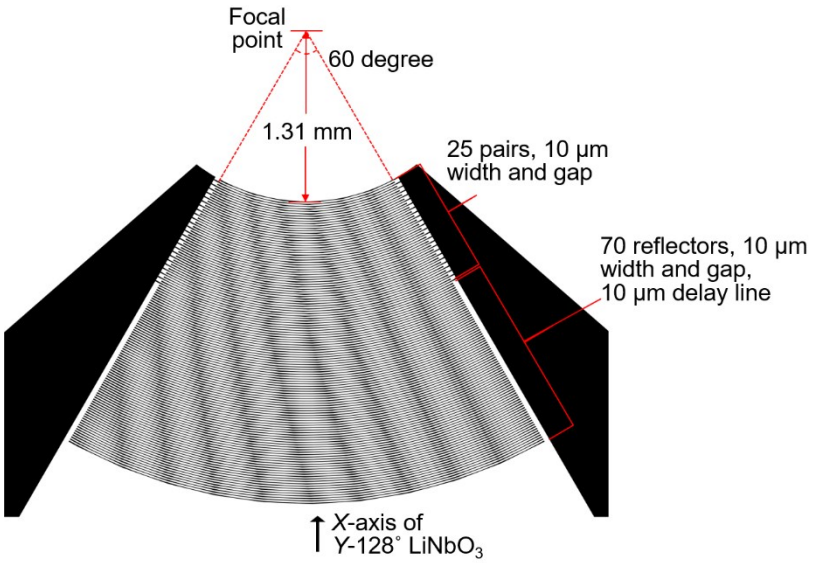

Figure S6. Detailed dimensions of the employed focused IDT for droplet coding.

Supplementary Movies

Supplementary Movie S1. On-demand dispensing of droplets at a speed of 20 Hz.

Supplementary Movie S2. On-demand dispensing of droplets at a speed of 40 Hz.

Supplementary Movie S3. On-demand dispensing of droplets at a speed of 100 Hz.

Supplementary Movie S4. Demonstration of automated measurement platform of flowing droplets.